# Acetylcholine Receptors in the Equatorial Region of Intrafusal Muscle Fibers Modulate Mouse Muscle Spindle Sensitivity

Laura Gerwin[1,2], Corinna Haupt[1], Katherine A. Wilkinson[3], Stephan Kröger[1]

[1] Department of Physiological Genomics, Biomedical Center, Ludwig-Maximilians-University, Großhaderner Str. 9, D-82152 Planegg-Martinsried, Germany

[2] Institute for Stem Cell Research, German Research Center for Environmental Health, Helmholtz Centre Munich, Ingolstädter Landstraße 1, D-85764 Neuherberg, Germany

[3] Department of Biological Sciences, San Jose State University, One Washington Square, San Jose, CA 95192, USA

Corresponding author: Stephan Kröger at above address

Email: skroeger@lmu.de

Phone: +49-89-2180-71899

Running title: AChR in muscle spindles

Key words: acetylcholine receptor, intrafusal fiber, proprioception, hemicholinium-3, d-tubocurarine, alpha-bungarotoxin

Key points summary:

- Acetylcholine receptors are aggregated in the central regions of intrafusal muscle fibers

- we recorded single unit muscle spindle afferent responses from isolated mouse EDL muscle in the absence of fusimotor input to ramp and hold stretches as well as to sinusoidal vibrations in the presence and absence of the acetylcholine receptor blockers d-tubocurarine and α-bungarotoxin

- proprioceptive afferent responses to both types of stretch were enhanced in the presence of either blocker

- blocking acetylcholine uptake and vesicular acetylcholine release by hemicholinium-3 also enhanced stretch-evoked responses

- these results represent the first evidence that acetylcholine receptors negatively modulate muscle spindle responses to stretch

- our data support the hypothesis that the sensory nerve terminal is able to release vesicles to fine-tune proprioceptive afferent sensitivity

**Abstract**

Muscle spindles are complex stretch-sensitive mechanoreceptors. They consist of specialized skeletal muscle fibers, called intrafusal fibers, which are innervated in the central (equatorial) region by afferent sensory axons and in both polar regions by efferent γ-motoneurons. Previously it was shown that acetylcholine receptors (AChR) are concentrated in the equatorial region at the contact site between the sensory neuron and the intrafusal muscle fiber. To address the function of these AChRs, single unit sensory afferents were recorded from an isolated mouse EDL muscle in the absence of γ-motoneuron activity. Specifically, we investigated the responses of individual sensory neurons to ramp-and-hold stretches and sinusoidal vibrations before and after the addition of the competitive and non-competitive AChR blockers d-tubocurarine or α-bungarotoxin, respectively. The presence of either drug did not affect the frequency of the resting action potential discharge frequency. However, the action potential frequencies in response to stretch were increased. In particular, frequencies of the dynamic peak and dynamic index to ramp and hold stretches were significantly higher in the presence of either drug. Treatment of muscle spindle afferents with the high-affinity choline transporter antagonist hemicholinium-3 similarly increased muscle spindle afferent firing frequencies during stretch. Moreover, the firing rate during sinusoidal vibration stimuli at low amplitudes was higher in the presence of α-bungarotoxin compared to control spindles also indicating an increased sensitivity to stretch. Collectively these data suggest a modulation of the muscle spindle afferent response to stretch by AChRs in the central region of intrafusal fibers possibly fine-tuning muscle spindle sensitivity.

## Introduction

Coordinated movements, including locomotion and their control, require proprioceptive information, i.e. information about muscle tone as well as position and movement of the extremities in space (Dietz, 2002). Muscle spindle afferents are the primary proprioceptive sensory receptors. They detect how much and how fast a muscle is lengthened (Proske & Gandevia, 2012; Kröger, 2018). Muscle spindle afferent feedback is required for a stable posture and directed movement but also for the realignment of fractured bones (Blecher *et al.*, 2017a), for the maintenance of spinal alignment (Blecher *et al.*, 2017b), and for basic locomotor recovery and circuit reorganization after spinal cord injury (Takeoka *et al.*, 2014). In adult mice, muscle spindles are 200-400 µm long and consist of 3-8 specialized intrafusal muscle fibers. Intrafusal fibers lie in parallel with extrafusal muscle fibers and are surrounded by a connective tissue capsule (Banks, 1994; Bewick & Banks, 2015; Kröger, 2018). Three types of intrafusal fibers can be distinguished: nuclear bag1, nuclear bag2 and nuclear chain fibers. Sensory neurons innervating bag1 fibers respond maximally to the velocity of changes in muscle fiber length (dynamic sensitivity) and those innervating bag2 fibers as well as nuclear chain fibers respond maximally to the amount of stretch (static sensitivity; Banks, 1994).

The central (equatorial) part of intrafusal muscle fibers is innervated by two types of afferent proprioceptive sensory neurons (termed “type Ia afferents” and “type II afferents” according to their axonal conduction velocity; Banks, 2015). Type Ia-afferents form so called annulospiral sensory nerve endings whereas type II-afferents flank the Ia-afferents (Schroder *et al.*, 1989; Sonner *et al.*, 2017). Afferent neurons generate action potentials with frequencies that are proportional to the size of the stretch and to the rate of stretching (De-Doncker *et al.*, 2003). The cell bodies of these sensory neurons constitute a minor fraction of all neurons in the dorsal root ganglion (DRG) and their peripheral endings can be labeled by antibodies against the vesicular glutamate transporter 1 (VGluT1; Wu *et al.*, 2004).

In addition to the sensory neurons, intrafusal muscle fibers are innervated by efferent γ-motoneurons, the so-called fusimotor innervation (Banks, 1994). These neurons constitute about 30 % of all motoneurons in the ventral horn of the spinal cord. Axons of γ-motoneurons enter the spindle together with the sensory fibers in the central region of the spindle but innervate intrafusal muscle fibers exclusively at both ends (polar regions) where they form a cholinergic synapse that appears functionally similar to the neuromuscular junction formed by α-motoneurons on extrafusal muscle fibers. Gamma-motoneurons adjust the sensitivity of muscle spindle afferents by inducing contraction in the polar region of the muscle spindle to exert tension on the central equatorial region of the muscle fiber (Proske, 1997; Banks, 1994).

This allows for continuous control of the mechanical sensitivity of spindles over the wide range of lengths and velocities that occur during normal motor behaviors. While the general functional properties of muscle spindles are rather well documented, the molecular basis of this function and potential modulatory activities remain mostly unknown (Kröger, 2018).

In a previous study, we analyzed the development of synapse-like specializations in muscle spindles (Zhang *et al.*, 2014). We reported a concentration of fetal (γ-subunit-containing) as well as adult (ε-subunit-containing) type AChRs in the equatorial region of intrafusal fibers at the contact site with the sensory nerve endings. Similarly, high concentrations of other proteins characteristic of cholinergic synapses, including the vesicular acetylcholine transporter, choline acetyltransferase and the AChR-associated protein rapsyn were detected at this nerve-to-muscle contact site (Zhang *et al.*, 2014). The function of these cholinergic specializations, however, remained unknown. In the present study, we analyzed the response of individual proprioceptive sensory afferent neurons to ramp-and-hold stretches as well as to sinusoidal vibrations in the presence and absence of a competitive (d-tubocurarine) or a non-competitive (α-bungarotoxin) AChR blocker. Moreover, we inhibited the high-affinity vesicular ACh transporter using hemicholinium-3. We show that all drugs increased muscle spindle sensitivity to stretch, demonstrating that AChRs in the central region of intrafusal muscle fibers modulate the sensitivity of muscle spindle sensory afferents.

## Methods

### Ethical Approval

Use and care of animals and all experimentation were approved by German authorities and according to national law (§7 TierSchG; license Az.: 55.2-1-54-2532.8-160-13) and conducted in accordance with the guidelines of the Ludwig-Maximilians-University. Experimental protocols were designed to minimize suffering and the number of animals used in the study. The authors declare that their work complies with the ethical principles under which *The Journal of Physiology* operates. At most five adult animals were housed in a sterile cage on a 12-hr light/dark cycle. A total of 19 male C57Bl/6JRj mice aged 10 – 15 weeks with a weight of 22-28 grams were used for the electrophysiological analyses. In the case of α-bungarotoxin and d-tubocurarine, five muscle spindles each from a different mouse were analyzed for each of the drug conditions. In the case of hemicholinium-3, four muscle spindle afferents, each from a different mouse, were recorded. In addition, we used five muscle spindle recordings, each from a different mouse, as controls. The values of the control group were compared to all three

drugs. The immunohistochemical analyses was performed on soleus, quadriceps and EDL muscles from three additional male C57Bl/6JRj mice.

Immunofluorescence

Immunofluorescence staining was performed as described previously (Zhang *et al.*, 2014). To obtain muscle tissue for immunohistochemistry, mice were deeply anesthetized using ketamine (Pfizer, Berlin, Germany) and xylazine (Bayer AG, Leverkusen, Germany). After transcardial perfusion with phosphate-buffered saline (PBS) followed by 4 % paraformaldehyde (PFA), the extensor digitorum longus muscle (EDL) was dissected. Muscles were post-fixed in 4 % PFA for 2 h and then incubated in 30 % sucrose in PBS overnight at 4 °C. Fixed muscles were cryo-preserved in Tissue-Tek O.C.T. Compound (Sakura Finetek Europe, AJ Alphen an den Rijn, Netherland) and cryo-sectioned along the longitudinal axis at 20-30 µm thickness.

Frozen sections were blocked in PBS containing 0.2 % Triton X-100 (Sigma-Aldrich Chemie GmbH, Taufkirchen, Germany) and 1 % bovine serum albumin (Carl Roth GmbH, Karlsruhe, Germany; blocking solution) for 30 min at room temperature and incubated with the primary antibody in blocking solution at 4 °C overnight. Sensory nerve terminals were stained using antibodies from guinea pig against the vesicular glutamate transporter 1 (VGluT1) diluted 1:1000 (AB5905, Millipore, Darmstadt, Germany). Primary antibodies were detected by incubating the sections for 1 h with Alexa647-conjugated donkey anti-guinea pig secondary antibody diluted 1:500 (AP1493SD, Millipore, Darmstadt, Germany). AChRs were visualized using Alexa488-conjugated α-bungarotoxin diluted 1:1000 in blocking solution (B13422, Life Technologies, Darmstadt, Germany). The nuclei were routinely stained using DAPI (Roth, Karlsruhe, Germany) at a concentration of 2 µg/ml in blocking solution.

After staining the sections were embedded in Mowiol mounting medium (Carl Roth, Karlsruhe, Germany) and analyzed using a Zeiss LSM 710 laser scanning confocal microscope (Carl Zeiss AG, Oberkochen, Germany). Sequentially scanned confocal Z-stacks of whole muscle spindles were obtained using 1µm optical sections and compiled using the ZEN2009 software (Zeiss). Laser power levels, photomultiplier gain levels, scanning speed, and the confocal pinhole size were kept constant between experimental and control specimens. Digital processing of entire images, including adjustment of brightness and contrast, was performed using the Java image processing program software package Fiji (Schindelin *et al.*, 2012).

Extracellular muscle spindle afferent recordings

Proprioceptive sensory neuron responses to stretch were assayed using an isolated muscle-nerve preparation as previously described (Wilkinson *et al.*, 2012; Franco *et al.*, 2014). Mice were sacrificed by cervical dislocation and the EDL muscle together with the deep peroneal branch of the sciatic nerve were dissected and placed in an oxygenated tissue bath containing artificial cerebrospinal fluid (ACSF; Wilkinson *et al.*, 2012). The tendons were sutured to a fixed post and on the other end to a lever arm, connected to a dual force and length controller (300C-LR, Aurora Scientific, Dublin, Ireland) allowing the simultaneous recording of muscle tension, muscle length and muscle spindle afferent discharges. Baseline muscle length (Lo) was defined as the length at which maximal twitch contractile force was generated. Sensory activity was sampled using a suction electrode (tip diameter 50–70 µm) which was connected to an extracellular amplifier (Model 1800, A&M Systems, Elkhart, Indiana, USA). A signal was classified as being from a putative muscle spindle sensory afferent if it displayed a characteristic instantaneous frequency response to stretch as well as a pause during twitch contraction (Wilkinson *et al.*, 2012). For every muscle spindle afferent recording, triplicates of ramp-and-hold stretches (Lo plus 7.5 % of Lo; ramp speed 40 % Lo $sec^{-1}$; stretch duration: 4 sec with 45 sec intervals between each stretch) were recorded and averaged. In addition, 16 sinusoidal vibrations (amplitudes: 5 µm, 10 µm, 50 µm, 100 µm, each with a frequency of 10 Hz, 25 Hz, 50 Hz, 100 Hz) were recorded for 9 sec and the values were expressed as impulses per 9 seconds (imp/9sec). Then, 30 µM d-tubocurarine (T2379, Sigma-Aldrich Chemie GmbH), 1.25 µM α-bungarotoxin (B1601, Life Technologies, Carlsbad, California, USA) or 30 µM hemicholinium-3 (HC-3; Sigma-Aldrich) was added to the oxygenated ACSF. At this concentration, α-bungarotoxin and tubocurarine completely inhibit neuromuscular transmission (Ganguly *et al.*, 1978; Chang *et al.*, 1989; Wenningmann & Dilger, 2001). For control measurements 100 µL ACSF were added instead of a drug. Initial control experiments showed no significant differences in the drug activity after equilibration times between 1 and 4 hrs. Therefore, an equilibration time of 1 hr for ACSF, d-tubocurarine and HC-3, respectively, and 3 hr for α-bungarotoxin were chosen. After equilibration, the response of the same muscle spindle afferent neuron to the same series of three repetitions of ramp-and-hold stretches and to the vibrations was determined. This allowed a precise comparison of the stretch-evoked responses of individual single unit muscle spindle afferents in the absence and presence of the drug. The resting discharge (average baseline firing rate) as well as the dynamic peak (highest firing rate during ramp – baseline firing rate), the dynamic index (dynamic peak – firing rate 0.45 to 0.55 sec into stretch – baseline firing rate) and the static response (firing rate 3.25 to

3.75 sec into stretch – baseline firing rate) and the time of silence (time after the end of the "ramp-and-hold" stretch and the first action potential) were determined (Wilkinson *et al.*, 2012; see Fig. 2).

For data analysis, individual sensory neurons were identified by spike shape and the interspike interval using the Spike Histogram feature of Lab Chart (AD Instruments, Sydney, Australia) and spindle afferent baseline firing rate, dynamic peak, dynamic index as well as the static stretch response were determined as described above. Only recordings in which an individual muscle spindle afferent unit could be unambiguously identified were included in the analysis. Action potentials from additional potential muscle spindles that appeared during the stretch were not scored. No attempt was made to discriminate type Ia from type II afferents (see Wilkinson et al., (2012) for a detailed discussion).

At the end of each recording, muscle health was ensured by determining the maximal contractile force during a direct tetanic stimulation with paddle electrodes embedded in the incubation chamber (500 ms train at 120 Hz frequency and 0.5 ms pulse length, supramaximal voltage; Grass S44 stimulator; Wilkinson *et al.*, 2012). The diameter of the EDL muscle was determined at Lo and with this information, the peak force was calculated and compared to the previously reported peak force of the EDL of 23,466 N/cm² (Larsson & Edstrom, 1986; Brooks & Faulkner, 1988). Neither the maximal directly-evoked muscle force after tetanic stimulation nor the resting spindle discharge varied significantly during the experimental period, suggesting that the spindle afferents were not undergoing time dependent changes in firing properties and that the muscle was returning to resting length following each stretch.

**Statistics**

Only single unit spindle afferent responses that could be recorded without interruption throughout the entire experiment, i.e. before and after the addition of either ACSF, d-tubocurarine, α-bungarotoxin or hemicholinium-3, were included in the analysis. For ramp and hold stretches, baseline values for all parameters (baseline firing rate, dynamic peak, dynamic index, and the static stretch response) were determined as an average of 3 stretches before drug addition. Likewise, post drug addition firing frequencies were determined after equilibration from an average of three stretches. Frequencies of individual muscle spindle afferents before drug addition were subtracted from the frequencies after drug addition. The same time points within a ramp-and-hold stretch were used to calculate the change in firing in our no drug control group. The mean of the overall changes in firing rate of all three drug groups were compared statistically using the one-way ANOVA (factor: drug) with Dunnett's post-hoc to the no drug

(ACSF) control group. Values are reported as mean of the frequency change from pre to post drug addition (Δmean; imp/sec) in a dot plot with each dot representing an individual muscle spindle afferent.

For the sinusoidal vibrations, the total number of action potentials per 9 seconds (imp/9sec) for each of the 4 frequencies and 4 amplitudes before drug addition were subtracted from the corresponding values (imp/9sec) after drug addition. Data are shown as Δ imp/9sec in a dot plot with each dot representing an independent experiment. Statistical significance was determined using the 3-way ANOVA (factors: drug, amplitude and frequency). Additionally, all the response to the 16 different vibrations in the absence and presence of all four drugs were compared individually with the one-way ANOVA (factor drug; Dunnett's multiple comparisons test). All analyses were performed using GraphPad Prism (v8; Graphpad Software, Inc., La Jolla, California, USA). The level of significance (p-value) for all statistical tests was set at * < 0.05, ** < 0.01, *** < 0.001.

**Results**

AChRs are concentrated at the equatorial region of the muscle spindle and colocalize with the sensory nerve terminal

Previously, the presence of mRNA coding for the α- and ε-subunit of the AChR in the central part of intrafusal fibers and the concentration of α-, γ- and ε-subunit containing AChRs at the contact site of the sensory nerve terminal and intrafusal muscle fibers was reported (Sanes *et al.*, 1991; Hippenmeyer *et al.*, 2002; Zhang *et al.*, 2014). To investigate the precise distribution of the AChRs with respect to the sensory nerve terminal, we analyzed sections stained with fluorescently labeled α-bungarotoxin and anti-VGluT1 antibodies. High-resolution confocal microscopic analyses of the central region of intrafusal muscle fibers demonstrated a precise codistribution of the AChRs with the VGluT1 immunoreactivity (Fig 1). A similar overall distribution of the AChR was observed in muscle spindles from EDL, quadriceps and soleus muscles (data not shown). As discussed previously (Zhang *et al.*, 2014), this labeling represents a concentration of the AChRs in the intrafusal fiber plasma membrane at the contact region with the sensory nerve terminal. Little α-bungarotoxin labeling was detected in the area of the intrafusal muscle fiber membrane between the annulospiral endings. A similar spatial distribution of AChRs was observed in nuclear bag and nuclear chain fibers from several different muscles. Based on the staining intensity, the concentration of the AChRs at the contact site between sensory neuron and intrafusal fiber appeared lower, compared to the

concentration of AChRs at neuromuscular junctions on extrafusal fibers or at γ-motoneuron endplates (data not shown).

D-tubocurarine, α-bungarotoxin and hemicholinium-3 increase stretch-evoked action potential frequencies of muscle spindle afferents

To investigate the function of the AChRs at the contact region between the sensory nerve terminal and the intrafusal muscle fiber, we analyzed individual muscle spindle afferent unit responses to a ramp-and-hold stretch (Lo plus 7.5 % of Lo; ramp speed 40 % Lo $sec^{-1}$; Fig. 2C), before (Fig. 2A) and after (Fig. 2B) the addition of two AChR blockers (d-tubocurarine and α-bungarotoxin, respectively) and an choline uptake inhibitor (hemicholinium-3). All drugs increased the firing frequency of stretch-evoked action potentials during ramp-and-hold stretches when compared to the frequencies of the same muscle spindle afferents before drug addition (Fig. 2E for α-bungarotoxin). Five different time points examining firing rates before, during and after the stretch were analyzed in detail (Fig. 2D). Analysis of the overall effect of the drugs using the one-way ANOVA (factor: drug) revealed no differences for the resting discharge (p-value: 0.0610), but statistically significant differences for the dynamic peak (p-value: 0.0100), dynamic index (p-value: 0.0204) and static response (p-value: 0.0459).

For better comparison of the specific effect of the individual drug, the results were expressed as Δmean, which represents the mean of the difference of the frequency (imp/sec) before compared to after drug addition. Neither AChR inhibitor had an effect on the resting discharge (Δmean control: 2.092 imp/sec; Δmean d-tubocurarine: 1.346 imp/sec; Δmean α-Btx: 4.758 imp/sec; Dunnett's post-hoc to ACSF control: p value (control vs. d-tubocurarine) = 0.9664; p value (control vs. α-Btx) = 0.4313; Figs. 2E, 3A) or the time silenced (data not shown). However, dynamic peak (Δmean control: -12.04 imp/sec; Δmean d-tubocurarine: 9.992 imp/sec; Δmean α-Btx: 26.53 imp/sec; Fig. 3B) and dynamic index (Δmean control: -5.413 imp/sec; Δmean d-tubocurarine: 2.78 imp/sec; Δmean α-Btx: 5.799 imp/sec; Fig. 3C) were increased compared to the same muscle spindle afferent before addition of the drug. The difference was statistically significant for the dynamic peak (p value (control vs. d-tubocurarine) = 0.0442; p value (control vs. α-Btx) = 0.0027; Fig. 3B) and for the dynamic index (p value (control vs. d-tubocurarine) = 0.0412; p value (control vs. α-Btx) = 0.0073; Fig. 3C). Alpha-bungarotoxin also significantly increased the static response (Δmean control: -5.581 imp/sec; Δmean α-Btx: 18.69 imp/sec; p value (control vs. α-Btx) = 0.0169; Fig. 3D). d-Tubocurarine did not affect the static response (Δmean d-tubocurarine: 8.276 imp/sec; p value

(control vs. d-tubocurarine) = 0.2122). Overall, our results demonstrate a higher sensitivity of muscle spindle responses to stretch in the presence of either AChR inhibitor.

Hemicholinium-3 (HC-3) is a blocker of the high-affinity uptake of choline into nerve terminals including the α-motoneuron terminal at the neuromuscular junction (Yu & Van der Kloot, 1991). Accordingly, application of HC-3 to neuromuscular junctions results in an inhibition of ACh synthesis and release (Carpenter & Woodruff, 1987). We used HC-3 to investigate if the blockade of vesicular acetylcholine uptake and release influenced the proprioceptive afferent responses to stretch. We observed no effect of HC-3 on the change of the action potential frequency before and after drug addition at rest (Δmean control: 2.092 imp/sec; Δmean HC-3: -1.612 imp/sec; p = 0.235; Fig. 3 A) and on the time silenced (not shown). This demonstrates that HC-3, similar to both AChR inhibitors, did not activate γ-motoneuron endplates and had no effect on muscle spindle sensory afferents at rest. However, in response to ramp-and-hold stretches the change of the frequency of muscle spindle afferents during the dynamic peak (Δmean control: -12.04 imp/sec; Δmean HC-3: 26.7 imp/sec; Fig. 3 B) and dynamic index (Δmean control: -5.413 imp/sec; Δmean HC-3: 16.35 imp/sec; Fig. 3C) were increased. The increase of the frequency was statistically significant (Dunnett's post-hoc to ACSF control; dynamic peak p = 0.0111; dynamic index p = 0.0071). We observed no effect of HC-3 on the static response (Δmean control: -5.581 imp/sec; Δmean HC-3: 8.867 imp/sec; static response p = 0.228; Fig. 3D). These results demonstrate that ACh uptake, synthesis and release modulate muscle spindle afferent firing rates in response to stretch.

The absolute values of the mean muscle spindle afferent frequencies before and after drug addition together with the corresponding standard deviations are given in Table 1. Comparing these values in the presence and absence of either drug revealed an increase in the response to stretch of approximately 20 % in the presence of either AChR inhibitor and of approximately 30% in the presence of HC-3. Collectively, our results demonstrate a role of AChRs during muscle spindle afferent responses to stretch and suggest a modulatory function for AChRs during proprioception.

Alpha-bungarotoxin increases muscle spindle responses during sinusoidal vibration stimuli

To analyze the function of the AChRs specifically during the dynamic response to stretch, we determined the effect of both AChR blockers and of HC-3 on muscle spindle afferent responses to sinusoidal vibrations varying in both displacement and frequency. Stimuli included four different frequencies (10, 25, 50 and 100 Hz) and four different amplitudes (5, 10, 50 and 100 μm). Compared to the ramp-and-hold stimuli, small amplitude sinusoidal vibrations test

dynamic responsiveness at much smaller length changes and, thus, provide more specific information about the dynamic sensitivity of muscle spindle afferents (Brown *et al.*, 1967). We observed an increase in the firing frequency in response to sinusoidal vibrations in the presence of all three drugs. Statistical analysis with the 3-way ANOVA (factors: drug, amplitude and frequency) showed that the change of the frequency before and after drug addition was statistically significant for the factor drug (p-value 0.0003) but not for the factors amplitude (p value = 0.6465) or frequency (p value = 0.0602). The effect was also significant for the drug by frequency analysis (p-value 0.0176) but not for the drug by amplitude (p value = 0.5672), amplitude by frequency (p value = 0.7768) or drug by amplitude and frequency analysis (p value = 0.522).

Additionally, each of the 16 vibrational stimuli was analyzed individually before and after drug addition with the one-way ANOVA and Dunnett's multiple comparison test. This analysis revealed that the frequencies were significantly increased in the presence of α-bungarotoxin particularly at high frequencies (50 and 100 Hz) and small amplitudes (5 and 10 µm; Fig. 4 B,C) but not at higher amplitudes (50 and 100 µm; Fig. 4 D,E) compared to the ACSF control. We observed no significant change in the presence of d-tubocurarine or HC-3 (Fig. 4 B-E). The absolute values (imp/9s ± standard deviation) for the responses to sinusoidal vibrations are shown in Table 2. In summary, the analysis of the effect of the drugs on muscle spindle afferent responses to vibrations further support a role for AChRs in modulating muscle spindle function during the dynamic phase of a stretch.

**Discussion**

In this study, we blocked AChR function using a non-competitive (α-bungarotoxin) as well as a competitive (d-tubocurarine) antagonist and tested the reaction of muscle spindles to stretch by using two different kinds of protocols, i.e. ramp-and-hold stretches and sinusoidal vibrations. During both kinds of stretch protocols, the action potential frequency was increased in the presence of either drug, whereas no change of the post-ramp time silenced, or in the discharge frequency at resting length was detectable. We observed a similar effect, i.e. increase in muscle spindle sensitivity during stretch, after inhibiting the high-affinity choline uptake system using HC-3. These results provide the first evidence for a function of AChRs in the equatorial region of the muscle spindle.

Several studies have previously analyzed the effect of cholinergic agonists and antagonists on muscle spindle firing (for review see Carr & Proske, 1996). For example,

application of cholinergic agents (including ACh, succinylcholine or nicotine) to muscle spindles induced strong excitatory activity in cat soleus muscle *in vivo*, which could be blocked by d-tubocurarine (Granit *et al.*, 1953; Albuquerque & Smith, 1964; Rack & Westbury, 1966; Smith & Albuquerque, 1967). This activity was concluded to be entirely due to a contraction of the polar regions of intrafusal fibers rather than activity acting directly on sensory nerve terminals. Likewise, intravenous injection of d-tubocurarine into anesthetized cats followed by fusimotor stimulation resulted in a small transient increase of the discharge frequencies in 55 %, a decrease in the frequencies in 29 % and an unchanged discharge frequency in 15 % of the cases during the first 20 minutes after d-tubocurarine administration (Smith & Albuquerque, 1967). In these and several other studies (reviewed by Carr & Proske, 1996), the drugs were either applied systemically for example by intravenous infusion, or their direct effect on stretch-evoked action potentials were not recorded. Therefore, these studies could not distinguish effects of the drugs at neuromuscular junctions on extrafusal fibers, γ-motoneuron endplates or AChRs in the central region of intrafusal fibers.

Our study differs from previous studies in several other aspects: We specifically analyzed the effect of antagonists instead of agonists. This excludes direct activation of AChRs at α- and γ-motoneuron endplates. We analyzed stretch-induced afferent changes instead of activity-induced by γ-motoneuron stimulation. This allowed the selective analysis of AChR function in the equatorial region of muscle fibers. Finally, we used single unit muscle spindle afferent recordings with a much higher sensitivity allowing us to detect small modulatory activities, which apparently have escaped detection in previous studies (Smith & Albuquerque, 1967; Ganguly *et al.*, 1978; Akoev, 1980).

Addition of d-tubocurarine, α-bungarotoxin or hemicholinium-3 did not change the resting discharge frequencies, strongly suggesting that neither drug directly activated γ-motoneuron endplates. In addition, the absence of an effect of either drug on the resting discharge levels makes a potential agonistic activity of d-tubocurarine on intrafusal muscle fibers unlikely (Takeda & Trautmann, 1984; Ziskind & Dennis, 1978). The effect of d-tubocurarine, α-bungarotoxin and hemicholinium-3 specifically on stretch-evoked responses also makes it unlikely that another sites of action of the drugs, including the sympathetic innervation (Santini & Ibata, 1971) or nociceptive fibers (Lund *et al.*, 2010b), affected our analysis. It is therefore very likely that we examined the effect of the drugs exclusively on the AChRs concentrated at the contact site between intrafusal muscle fibers and proprioceptive sensory neuron.

Since all drugs caused an increase in the dynamic as well as in the static response to stretch, all three types of intrafusal fibers are likely to be affected. In agreement with this hypothesis, AChRs were detected at the contact site between sensory neuron and nuclear bag as well as nuclear chain fibers. However, more refined experiments are needed to specifically distinguish if the drugs affect all three different intrafusal fiber types to the same extent.

The effect of α-bungarotoxin on muscle spindle responses to ramp-and-hold stretches as well as to vibrations was stronger compared to the effect of d-tubocurarine. For example, α-bungarotoxin affected the static response and small amplitude vibrations, whereas d-tubocurarine did not. It is unlikely that we used non-saturating conditions of either AChR inhibitor, since increasing the concentration of α-bungarotoxin or d-tubocurarine did not affect muscle spindle responses. One potential explanation is that both drugs affect the fetal and adult AChR, which are both concentrated in the central region of intrafusal fibers (Zhang *et al.*, 2014), to a different extent. It has previously been shown that d-tubocurarine is 6-fold less effective in blocking ACh-elicited current from fetal AChR compared to α-bungarotoxin (Kopta & Steinbach, 1994). This reduced efficacy in blocking the fetal AChR might be sufficient to reduce the effect of d-tubocurarine below statistical significance.

Previous studies have shown that in addition to the AChR, the acetylcholine receptor-associated protein rapsyn is concentrated in the equatorial region precisely at the contact site of the intrafusal fiber and the sensory neuron (Zhang *et al.*, 2014), suggesting a similar anchoring of the AChR in the subsarcolemmal cytoskeleton as at the neuromuscular junction. The sensory nerve terminals also contain the vesicular acetylcholine transporter and choline acetyl transferase, the key enzyme of acetylcholine synthesis (Zhang *et al.*, 2014). In addition, synaptic-like vesicles (Bewick *et al.*, 2005) and molecules required for their exocytosis can be detected in sensory nerve terminals. These include the presynaptic cytomatrix protein bassoon, the vesicle clustering protein synapsin I, as well as synaptophysin, synaptotagmin, VAMP/synaptobrevin I and II, as well as syntaxin (Aguado *et al.*, 1999; De Camilli *et al.*, 1988; Li *et al.*, 1996; Bewick *et al.*, 2005; Simon *et al.*, 2010; Zhang *et al.*, 2014; Bewick, 2015). In addition, previous studies using the styryl dye FM1-43 demonstrated vesicle exo- and endocytosis within the sensory nerve terminal (Banks *et al.*, 2002; Bewick *et al.*, 2005). This vesicle turnover was increased 4-fold in response to stretch and depended on the presence of extracellular calcium ions (Bewick *et al.*, 2005). Collectively, these previously published results together with the present study suggest that the terminals of the stretch-sensitive muscle spindle afferents have molecular specializations reminiscent of cholinergic synapses and contain the molecular machinery required to release synapse-like vesicles.

The high-affinity choline transporter is essential for proper signaling at cholinergic synapses, including the neuromuscular junction, due to the transporter's rate-limiting reuptake of choline that is required to sustain ACh synthesis and release (Carpenter & Woodruff, 1987; Ferguson *et al.*, 2004; Lund *et al.*, 2010a). Accordingly, treatment of neuromuscular junctions with the high-affinity choline transporter antagonist hemicholinium-3 reduced the level of ACh in presynaptic vesicles suggesting that this drug leads to an impaired ability to maintain an adequate amount of releasable pools of ACh (Yu & Van der Kloot, 1991). We demonstrate that incubation of muscle spindles with hemicholinium-3 resulted in an increase in the firing frequencies during the dynamic peak and dynamic index by about 30 %. Thus, the effect of blocking AChRs in the central region of intrafusal fibers or inhibiting ACh uptake into the sensory nerve terminal were similar, further supporting the hypothesis that the ACh-mediated signaling is part of a stretch-dependent modulatory feedback system regulating muscle spindle sensitivity. Since at the neuromuscular junction more than 90% of the HC-3-sensitive high-affinity choline transporter is present on synaptic vesicles (Nakata *et al.*, 2004) and since the high-affinity choline uptake is rate limiting to ACh synthesis and its release (Ferguson *et al.*, 2004), our results are also consistent with a vesicular release of acetylcholine from sensory neurons.

As discussed in detail previously (Zhang *et al.*, 2014), several lines of evidence strongly suggest that AChRs in the central region of intrafusal fibers are concentrated in the muscle fiber plasma membrane, rather than in the sensory nerve terminal. Thus, it appears likely that α-bungarotoxin and d-tubocurarine affect AChRs located in the plasma membrane of intrafusal fibers rather than in the sensory nerve terminal. Based on the results of the present study, we propose that some vesicles in the sensory nerve terminal contain acetylcholine. The stretch-dependent release of this ACh could activate AChRs in the intrafusal muscle fiber membrane directly opposite to the sensory nerve terminal. If this release is calcium-dependent (Bewick *et al.*, 2005) and involves the stretch-sensitive calcium channel, which has been described in the sensory nerve terminal (Hunt et al., 1978; Kruse & Poppele, 1991), or the Piezo2 channel (Woo *et al.*, 2015), is currently unknown. Since we did not observe an effect of d-tubocurarine or of α-bungarotoxin on the firing rate of resting muscle spindles, we assume that acetylcholine is released primarily during mechanical activity. This was unexpected since at least some glutamate-containing vesicles are released constitutively (Bewick *et al.*, 2005). Our results are therefore consistent with the possibility that both neurotransmitters are stored within separate populations of vesicles. However, future studies are needed to further characterize the

glutamate- and ACh-containing vesicle populations and their modulation of muscle spindle sensitivity.

Binding of sensory neuron-derived acetylcholine to the AChR would most likely result in a depolarization of the intrafusal fiber due to cation influx via the AChR. If this leads to a graded potential or to an action potential is unknown. In any case, since nuclear bag- and nuclear chain fibers contain a cylinder of myofilaments directly underneath the plasma membrane in their equatorial region (see for example Ovalle, 1972), the AChR-mediated depolarization could lead to a contraction of the sarcomeres in the central part of the intrafusal muscle fibers. The function of this contraction, however, remains speculative. In principle, a contraction of sarcomeres in the equatorial region would lead to a lengthening of the polar regions and to a reduced sensitivity to stretch of the equatorial region. Alternatively, the AChR-mediated depolarization in the equatorial region could sum up with the graded potentials or action potentials induced by γ-motoneuron activity in the polar regions leading to an even stronger contraction. Thus, the mechanism how AChRs in the equatorial region modulate the stretch-induced muscle spindle afferent firing rate during stretch remains unclear and, clearly, more experiments are needed to substantiate this hypothesis. In any case, our results further support the idea that in addition to sending afferent information about muscle length changes to the central nervous system, muscle spindle afferent terminals also release neurotransmitters that may control intrafusal fiber tone.

A termination of the AChR activation could be mediated by acetylcholinesterase, although there have been conflicting results regarding the presence of this enzyme in the central region of intrafusal fibers (Giacobini, 1959; Schober & Thomas, 1978; Zhang *et al.*, 2014). Alternatively, a long-lasting presence of ACh (due to the absence of AChE in the central region of intrafusal fibers) might generate a background intrafusal muscle fiber tone, counteracting the mechanical tension generated by the fusimotor activity in the polar regions.

Proprioceptive sensory afferents contain glutamate-filled synapse-like vesicles suggesting that they might release glutamate. This glutamate might, via an unusual phospholipase D-linked metabotropic glutamate receptor within the sensory nerve terminal, enhance stretch-induced sensory afferent excitability (Bewick *et al.*, 2005; Simon *et al.*, 2010; Bewick & Banks, 2015; Bewick, 2015). The results from our study suggest that ACh has a different effect. In contrast to glutamate, ACh is likely to modulate only stretch-induced responses via the nicotinic AChRs in the intrafusal muscle fiber plasma membrane. Moreover, ACh acts as a negative modulator, reducing stretch-induced sensitivity. Our results extend the

possibility that mechanical activity releases glutamate- to include ACh-containing vesicles, too, and that both modulate the proprioceptive sensory neuron's response to stretch.

## References


Aguado F, Majo G, Ruiz-Montasell B, Llorens J, Marsal J & Blasi J. (1999). Syntaxin 1A and 1B display distinct distribution patterns in the rat peripheral nervous system. *Neuroscience* **88,** 437-446.

Akoev GN. (1980). Catecholamines, acetylcholine and excitability of mechanoreceptors. *Prog Neurobiol* **15,** 269-294.

Albuquerque EX & Smith CM. (1964). Specificity of Excitation of Muscle Spindle Afferents by Cholinergic Substances. *J Pharmacol Exp Ther* **146,** 344-353.

Banks RW. (1994). The motor innervation of mammalian muscle-spindles. *Prog Neurobiol* **43,** 323-362.

Banks RW. (2015). The innervation of the muscle spindle: a personal history. *J Anat* **227,** 115-135.

Banks RW, Bewick GS, Reid B & Richardson C. (2002). Evidence for activity-dependent modulation of sensory-terminal excitability in spindles by glutamate release from synaptic-like vesicles. *Adv Exp Med Biol* **508,** 13-18.

Bewick GS. (2015). Synaptic-like vesicles and candidate transduction channels in mechanosensory terminals. *J Anat* **227,** 194-213.

Bewick GS & Banks RW. (2015). Mechanotransduction in the muscle spindle. *Eur J Physiol* **467,** 175-190.

Bewick GS, Reid B, Richardson C & Banks RW. (2005). Autogenic modulation of mechanoreceptor excitability by glutamate release from synaptic-like vesicles: evidence from the rat muscle spindle primary sensory ending. *J Physiol* **562,** 381-394.

Blecher R, Krief S, Galili T, Assaraf E, Stern T, Anekstein Y, Agar G & Zelzer E. (2017a). The proprioceptive system regulates morphologic restoration of fractured bones. *Cell reports* **20,** 1775-1783.

Blecher R, Krief S, Galili T, Biton IE, Stern T, Assaraf E, Levanon D, Appel E, Anekstein Y, Agar G, Groner Y & Zelzer E. (2017b). The proprioceptive system masterminds spinal alignment: Insight into the mechanism of scoliosis. *Dev Cell* **42,** 388-399 e383.

Brooks SV & Faulkner JA. (1988). Contractile properties of skeletal muscles from young, adult and aged mice. *J Physiol* **404,** 71-82.

Brown MC, Engberg I & Matthews PB. (1967). The relative sensitivity to vibration of muscle receptors of the cat. *J Physiol* **192,** 773-800.

Carpenter FG & Woodruff CR. (1987). Blockade and recovery of cholinergic transmission in rats treated with hemicholinium 3. *Eur J Pharmacol* **141,** 179-186.

Carr RW & Proske U. (1996). Action of cholinesters on sensory nerve endings in skin and muscle. *Clin Exp Pharmacol Physiol* **23,** 355-362.

Chang CC, Chiou LC & Hwang LL. (1989). Selective antagonism to succinylcholine-induced depolarization by alpha-bungarotoxin with respect to the mode of action of depolarizing agents. *Br J Pharmacol* **98,** 1413-1419.

De-Doncker L, Picquet F, Petit J & Falempin M. (2003). Effects of hypodynamia-hypokinesia on the muscle spindle discharges of rat soleus muscle. *J Neurophysiol* **89,** 3000-3007.

De Camilli P, Vitadello M, Canevini MP, Zanoni R, Jahn R & Gorio A. (1988). The synaptic vesicle proteins synapsin I and synaptophysin (protein P38) are concentrated both in efferent and afferent nerve endings of the skeletal muscle. *J Neurosci* **8,** 1625-1631.

Dietz V. (2002). Proprioception and locomotor disorders. *Nature Rev Neurosci* **3,** 781-790.

Ferguson SM, Bazalakova M, Savchenko V, Tapia JC, Wright J & Blakely RD. (2004). Lethal impairment of cholinergic neurotransmission in hemicholinium-3-sensitive choline transporter knockout mice. *Proc Natl Acad Sci U S A* **101,** 8762-8767.

Franco JA, Kloefkorn HE, Hochman S & Wilkinson KA. (2014). An in vitro adult mouse muscle-nerve preparation for studying the firing properties of muscle afferents. *J Vis Exp* **91,** 51948.

Ganguly DK, Nath DN, Ross HG & Vedasiromoni JR. (1978). Rat isolated phrenic nerve-diaphragm preparation for pharmacological study of muscle spindle afferent activity: effect of oxotremorine. *Br J Pharmacol* **64,** 47-52.

Giacobini E. (1959). Quantitative determination of cholinesterase in individual spinal ganglion cells. *Acta Physiol Scand* **45,** 238-254.

Hippenmeyer S, Shneider NA, Birchmeier C, Burden SJ, Jessell TM & Arber S. (2002). A role for neuregulin1 signaling in muscle spindle differentiation. *Neuron* **36,** 1035-1049.

Hunt CC, Wilkinson RS & Fukami Y. (1978). Ionic basis of the receptor potential in primary endings of mammalian muscle spindles. *J Gen Physiol* **71,** 683-698.

Kopta C & Steinbach JH. (1994). Comparison of mammalian adult and fetal nicotinic acetylcholine receptors stably expressed in fibroblasts. *J Neurosci* **14**, 3922-3933.

Kröger S. (2018). Proprioception 2.0: novel functions for muscle spindles. *Curr Opin Neurol* **31,** 592-598.

Kruse MN & Poppele RE. (1991). Components of the dynamic response of mammalian muscle spindles that originate in the sensory terminals. *Exp Brain Res* **86,** 359-366.

Larsson L & Edstrom L. (1986). Effects of age on enzyme-histochemical fibre spectra and contractile properties of fast- and slow-twitch skeletal muscles in the rat. *J Neurol Sci* **76,** 69-89.

Li JY, Edelmann L, Jahn R & Dahlstrom A. (1996). Axonal transport and distribution of synaptobrevin I and II in the rat peripheral nervous system. *J Neurosci* **16,** 137-147.

Lund D, Ruggiero AM, Ferguson SM, Wright J, English BA, Reisz PA, Whitaker SM, Peltier AC & Blakely RD. (2010a). Motor neuron-specific overexpression of the presynaptic

choline transporter: impact on motor endurance and evoked muscle activity. *Neuroscience* **171,** 1041-1053.

Lund JP, Sadeghi S, Athanassiadis T, Caram Salas N, Auclair F, Thivierge B, Arsenault I, Rompre P, Westberg KG & Kolta A. (2010b). Assessment of the potential role of muscle spindle mechanoreceptor afferents in chronic muscle pain in the rat masseter muscle. *PloS one* **5,** e11131.

Nakata K, Okuda T & Misawa H. (2004). Ultrastructural localization of high-affinity choline transporter in the rat neuromuscular junction: enrichment on synaptic vesicles. *Synapse* **53,** 53-56.

Ovalle WK, Jr. (1972). Fine structure of rat intrafusal muscle fibers. The equatorial region. *J Cell Biol* **52,** 382-396.

Proske U. (1997). The mammalian muscle spindle. *News Physiol Sci* **12,** 37-42.

Proske U & Gandevia SC. (2012). The proprioceptive senses: their roles in signaling body shape, body position and movement, and muscle force. *Physiol Rev* **92,** 1651-1697.

Rack PM & Westbury DR. (1966). The effects of suxamethonium and acetylcholine on the behaviour of cat muscle spindles during dynamics stretching, and during fusimotor stimulation. *J Physiol* **186,** 698-713.

Sanes JR, Johnson YR, Kotzbauer PT, Mudd J, Hanley T, Martinou JC & Merlie JP. (1991). Selective expression of an acetylcholine receptor-lacZ transgene in synaptic nuclei of adult muscle fibers. *Development* **113,** 1181-1191.

Santini M & Ibata Y. (1971). The fine structure of thin unmyelinated axons within muscle spindles. *Brain Res* **33,** 289-302.

Schindelin J, Arganda-Carreras I, Frise E, Kaynig V, Longair M, Pietzsch T, Preibisch S, Rueden C, Saalfeld S, Schmid B, Tinevez JY, White DJ, Hartenstein V, Eliceiri K, Tomancak P & Cardona A. (2012). Fiji: an open-source platform for biological-image analysis. *Nature Meth* **9,** 676-682.

Schober R & Thomas E. (1978). The fine structural localization of acetylcholinesterase in the muscle spindle of the rat. *Cell Tissue Res* **186,** 39-52.

Schröder JM, Bodden H, Hamacher A & Verres C. (1989). Scanning electron microscopy of teased intrafusal muscle fibers from rat muscle spindles. *Muscle Nerve* **12,** 221-232.

Simon A, Shenton F, Hunter I, Banks RW & Bewick GS. (2010). Amiloride-sensitive channels are a major contributor to mechanotransduction in mammalian muscle spindles. *J Physiol* **588,** 171-185.

Smith CM & Albuquerque EX. (1967). Differences in the tubocurarine antagonism of the activation of muscle spindle afferents by siccinylcholine, acetylcholine and nicotine. *J Pharmacol Exp Ther* **156,** 573-584.

Sonner MJ, Walters MC & Ladle DR. (2017). Analysis of proprioceptive sensory innervation of the mouse soleus: A whole-mount muscle approach. *PloS one* **12,** e0170751.

Takeda K & Trautmann A. (1984). A patch-clamp study of the partial agonist actions of tubocurarine on rat myotubes. *J Physiol* **349,** 353-374.

Takeoka A, Vollenweider I, Courtine G & Arber S. (2014). Muscle spindle feedback directs locomotor recovery and circuit reorganization after spinal cord injury. *Cell* **159,** 1626-1639.

Wenningmann I & Dilger JP. (2001). The kinetics of inhibition of nicotinic acetylcholine receptors by (+)-tubocurarine and pancuronium. *Mol Pharmacol* **60,** 790-796.

Wilkinson KA, Kloefkorn HE & Hochman S. (2012). Characterization of muscle spindle afferents in the adult mouse using an in vitro muscle-nerve preparation. *PloS one* **7,** e39140.

Woo SH, Lukacs V, de Nooij JC, Zaytseva D, Criddle CR, Francisco A, Jessell TM, Wilkinson KA & Patapoutian A. (2015). Piezo2 is the principal mechanotransduction channel for proprioception. *Nat Neurosci* **18,** 1756-1762.

Wu SX, Koshimizu Y, Feng YP, Okamoto K, Fujiyama F, Hioki H, Li YQ, Kaneko T & Mizuno N. (2004). Vesicular glutamate transporter immunoreactivity in the central and peripheral endings of muscle-spindle afferents. *Brain Res* **1011,** 247-251.

Yu SP & Van der Kloot W. (1991). Increasing quantal size at the mouse neuromuscular junction and the role of choline. *J Physiol* **433,** 677-704.

Zhang Y, Wesolowski M, Karakatsani A, Witzemann V & Kröger S. (2014). Formation of cholinergic synapse-like specializations at developing murine muscle spindles. *Dev Biol* **393,** 227-235.

Ziskind L & Dennis MJ. (1978). Depolarising effect of curare on embryonic rat muscles. *Nature* **276,** 622-623.

## Author contributions

Conception and design of the work: S.K. and K.A.W. conceived the project and designed the experiments. L.G. and C.H. performed, analyzed, and interpreted the experiments. S.K. wrote the first draft of the manuscript. All authors revised the manuscript and approved the final version submitted for publication. All authors agreed to be accountable for all aspects of the work in ensuring that questions related to the accuracy or integrity of any part are appropriately investigated and resolved. All persons designated as authors qualify for authorship, and all those who qualify for authorship are listed as authors. All authors declare no conflict of interest.

## Funding

The work was supported by grants from the Deutsche Forschungsgemeinschaft (DFG; grant KR1039/16-1), the Friedrich-Baur-Association, and the Deutsche Gesellschaft für Muskelkranke (DGM). We are particularly grateful to the Graduate School of Systemic Neuroscience Munich (GSN) and the Munich Center for NeuroSciences – Brain and Mind (MCN) for their generous financial support.

## Acknowledgement

We would like to thank Hansruedi Brenner and Peter Grafe for many helpful discussions, Peter Fischer and Veit Witzemann for donating equipment, Martina Bürkle for expert technical assistance, Magdalena Götz for constant support and encouragement, Richard Carr, Guy Bewick, Bob Banks and Hansruedi Brenner for carefully reading and improving the manuscript. We would also like to thank both reviewers for their critical but insightful comments.

**Figure legends:**

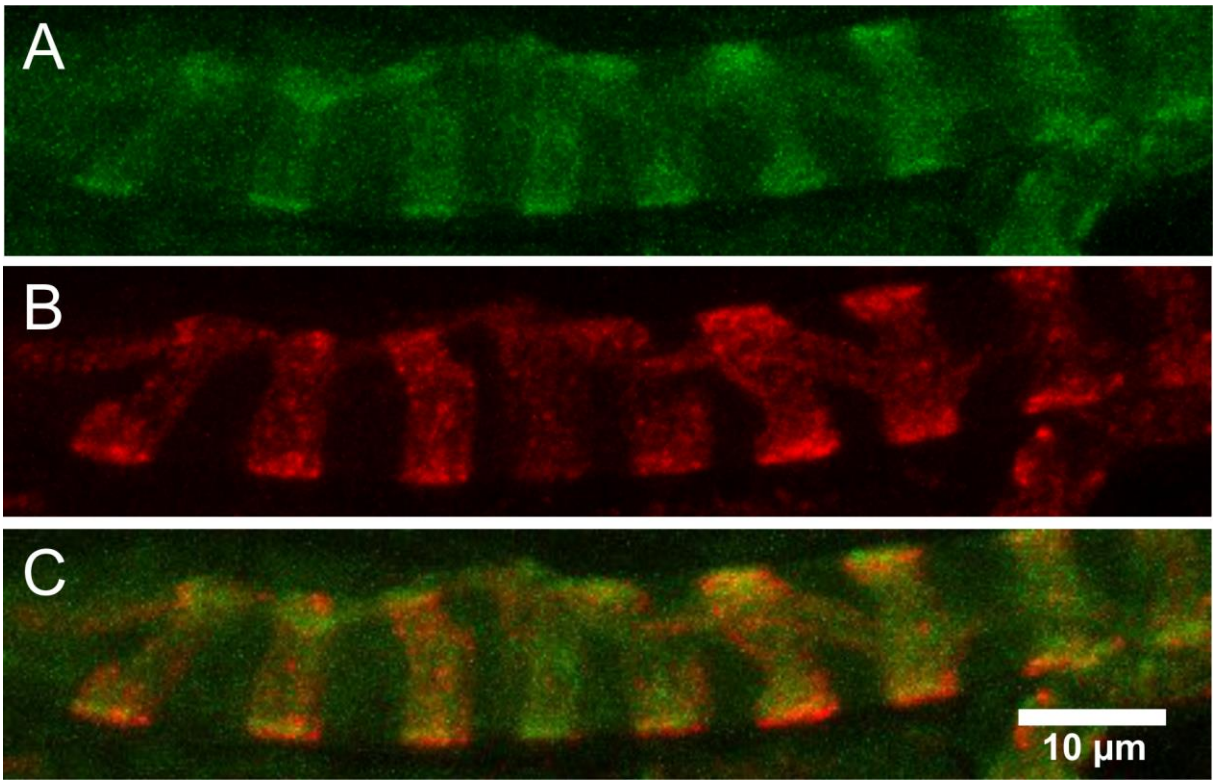


**Figure 1:** AChRs and sensory nerve terminals colocalize in the central region of muscle spindles. High-resolution confocal z-scan of the distribution of the AChR (green channel, panel A) and the sensory nerve terminal indicated by anti-VGluT1 immunoreactivity (red channel, panel B) in the central region of a nuclear chain fiber of a soleus muscle is shown. Note the precise overlap of both staining patterns and the concentration of AChR labeling at the contact site between sensory neuron and intrafusal muscle fiber (panel C).

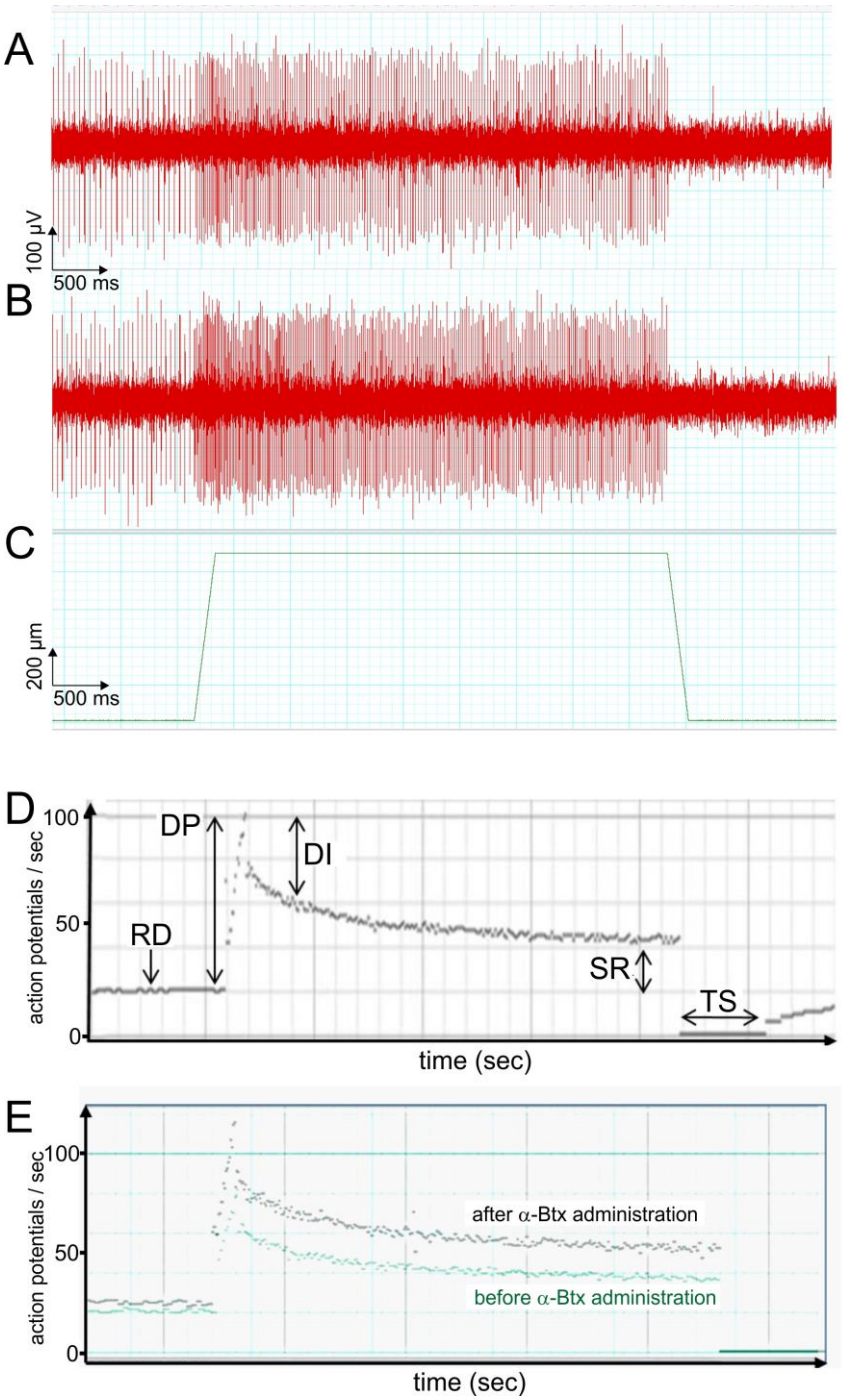


**Figure 2:** Inhibition of AChRs increases stretch-evoked sensory afferent instantaneous frequencies. Action potentials of the same muscle spindle proprioceptive afferent during a ramp-and-hold stretch in the absence (panel A) and presence (panel B) of α-bungarotoxin. Panel C shows a ramp-and-hold stimulus of four seconds with a ramp speed of 40 % Lo $sec^{-1}$ and an overall 7.5 % Lo length change of the same spindle as in panels A and B. Panel D shows the response of a different muscle spindle afferent to stretch to illustrate the five different parameters that were analyzed at different time points before, during and after the stretch: resting discharge (RD), dynamic peak (DP), dynamic index (DI), static response (SR) and time silenced (TS). Panel E shows a representative image of the instantaneous frequency of a single proprioceptive sensory unit response to stretch before (green dots) and after the addition of α-bungarotoxin (α-Btx; grey dots). The presence of α-bungarotoxin did not influence the resting discharge (the small variability shown in panel E is not significant), but increased the instantaneous frequencies at all other time points during the stretch.

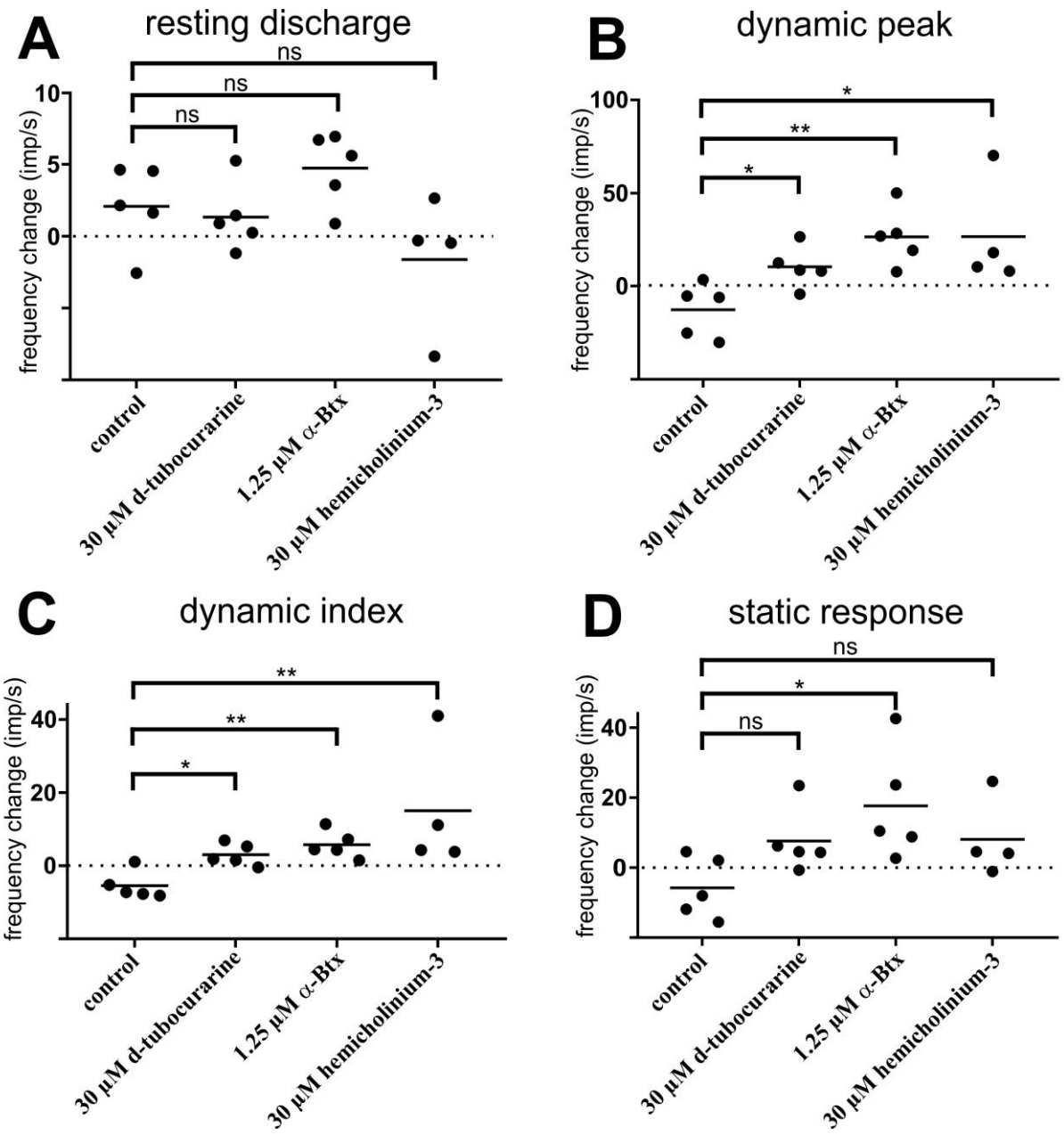


**Figure 3:** d-Tubocurarine, α-bungarotoxin and hemicholinium-3 have no effect on resting discharge frequencies but increase the firing rate during ramp-and-hold stretches. The effect of stretches of 7.5 % of Lo on single unit proprioceptive afferents was determined before and after addition of d-tubocurarine, α-bungarotoxin or hemicholinium-3. Each dot represents the change of the instantaneous frequency (impulses per second) of a single muscle spindle afferent unit where the impulses before drug addition were subtracted from the values after drug addition. The mean of the change is indicated as horizontal line. Five spindles, each from a different mouse, were evaluated in the presence and absence of a-bungarotoxin and d-tubocurarine, respectively (N=5). Four mice were evaluated in the presence and absence of hemicholinium-3 (N=4). Control values represent muscle spindle activities where ACSF was added instead of a drug. Addition of either drug increased the firing frequencies during the dynamic peak (B) and the dynamic index (C) whereas the resting discharge frequency (A) remained unchanged. Alpha-bungarotoxin also affected the static response (D). Statistical significance was evaluated using the one-way ANOVA (factor: drug) with Dunnett's post hoc corrections. The small increase (panel A) or decrease (panel B-D) of the control frequency after ACSF addition compared to the frequency before ACSF addition was not statistically significant.

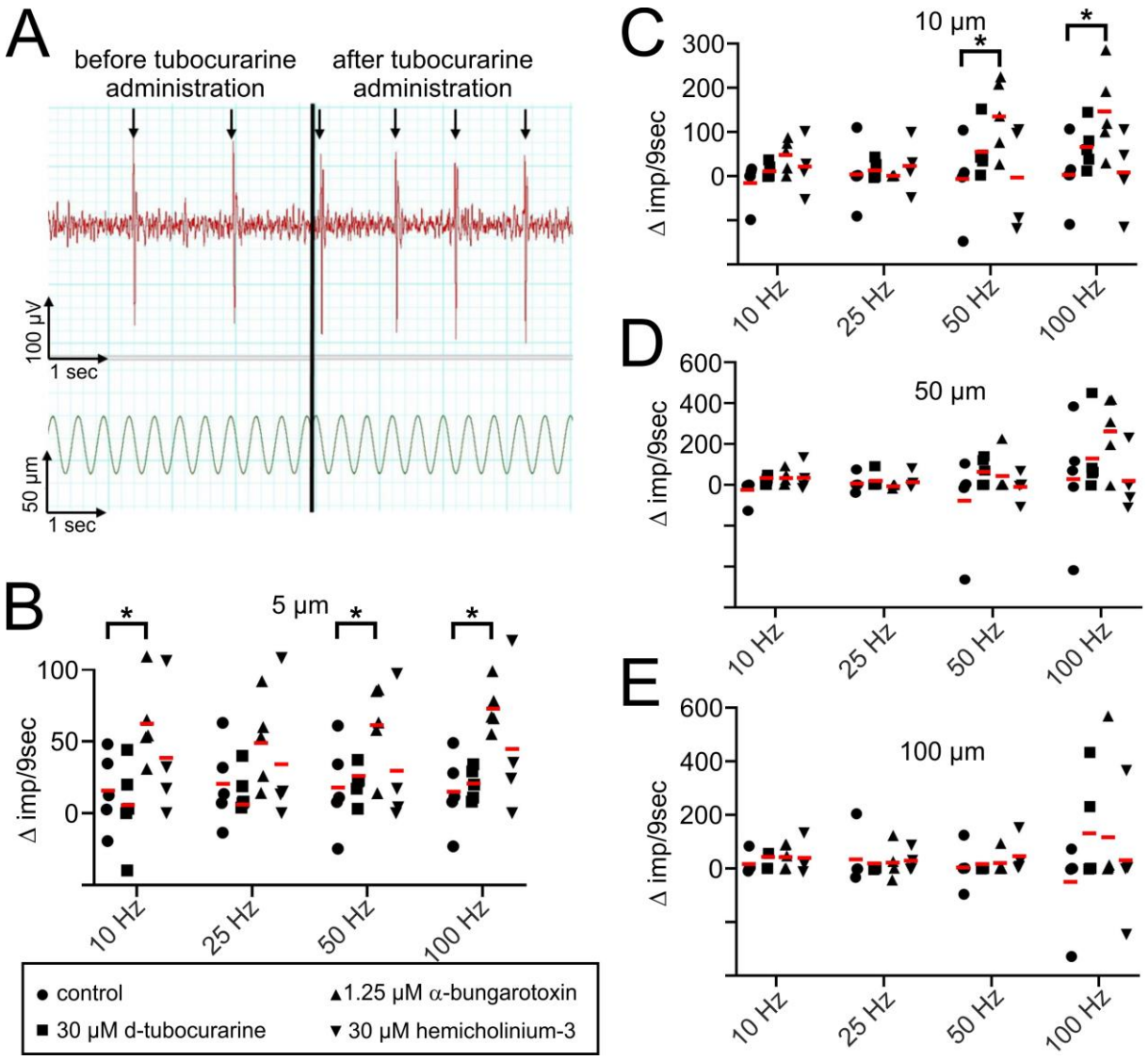


**Figure 4:** Response of muscle spindle sensory afferents to sinusoidal vibration stimuli in the presence and absence of cholinergic inhibitors. Panel A shows individual action potentials of a representative muscle spindle afferent in response to sinusoidal length changes displayed below (stretch is represented as upwards deflection). While in the absence of any drug (left side), this muscle spindle afferent entrained with every 4$^{th}$ vibration, addition of d-tubocurarine (right side of panel A) increased the firing frequency so that entrainment was observed every second to third vibration. Quantification of sixteen different sinusoidal vibration stimuli (5, 25, 50 and 100 µm amplitude with each with frequencies of 10 Hz, 25 Hz, 50 Hz, and 100 Hz, respectively) are shown in panels B – E. Each dot represents the difference of the impulses per 9 seconds (Δ imp/9 sec) where the values before drug (or ACSF in the case of controls) addition were subtracted from those after drug addition. The mean of the 5 (ACSF, α-bungarotoxin or d-tubocurarine) or 4 (hemicholinium-3) individual experiments is indicated as red line. Asterisks represent statistically significant differences between the muscle spindles before and after addition of the drug, as determined using the one-way ANOVA (factor: drug) with Dunnett's post-hoc to the no drug control group. The non-normalized values for each condition ± standard deviation are shown in Table 2. Note the increased firing frequencies in the presence of α-bungarotoxin particularly at small amplitudes and high frequencies.

**Table 1:** Original values (frequencies in imp/sec) of the mean responses to ramp-and-hold stretches used to determine the Δmean in Fig. 3. The numbers represent the mean ± standard deviation with N=5 for control, α-bungarotoxin and d-tubocurarine and N=4 for HC-3.

**Table 2:** Original values (impulses per 9 sec) of the mean responses of muscle spindle afferents to sinusoidal vibrations of different amplitudes and frequencies. The values were used to determine the frequency change in percent in Fig. 4 B-E. The numbers represent the mean ± standard deviation with N=5 for control (ACSF), α-bungarotoxin and d-tubocurarine and N=4 for HC-3.

**Table 1**

| MEAN (imp/sec) | | | | | | | | |
|---|---|---|---|---|---|---|---|---|
| | control | | α-bungarotoxin | | d-tubocurarine | | HC-3 | |
| | before | after | before | after | before | after | before | after |
| RD | 13,0 ± 6,0 | 15,1 ± 5,8 | 18,4 ± 4,4 | 23,2 ± 5,8 | 16,4 ± 3,6 | 17,8 ± 2,4 | 20,8 ± 1,5 | 19,2 ± 2,8 |
| DP | 94,2 ± 20,6 | 88,0 ± 31,5 | 56,8 ± 21,6 | 83,3 ± 34,5 | 60,5 ±23,5 | 70,5 ± 7,8 | 50,5 ± 14,7 | 77,2 ± 12,8 |
| DI | 37,3 ± 9,3 | 34,2 ± 11,6 | 27,9 ± 10,3 | 33,7 ± 10,4 | 27,3 ± 8,6 | 30,1 ± 9,2 | 26,1 ± 5,3 | 42,5 ± 5,4 |
| SR | 42,2 ± 12,9 | 40,3 ± 18,3 | 17,7 ± 7,4 | 36,4 ± 22,9 | 21,5 ±10,5 | 29,8 ±16,2 | 15,6 ± 1,8 | 24,4 ± 5,5 |

**Table 2**

| **control** | | | | | |
|---|---|---|---|---|---|
| | | **amplitude** | | | |
| **frequency** | | 5 µm | 10 µm | 50 µm | 100 µm |
| 10 Hz | before | 119,5 ± 61,6 | 148,3 ± 80,2 | 155,9 ± 83,8 | 176,3 ± 56,7 |
| | after | 135,2 ± 49,6 | 133,8 ± 46,8 | 130,4 ± 42,7 | 191,6 ± 60,1 |
| 25 Hz | before | 122,9 ± 65,4 | 207,5 ± 68,1 | 221,5 ± 39,1 | 234,5 ± 13,4 |
| | after | 143,2 ± 58,2 | 211,8 ± 26,4 | 229,4 ± 8,3 | 267,6 ± 76,9 |
| 50 Hz | before | 125,2 ± 67,5 | 241,4 ± 89,6 | 433,2 ± 257,1 | 448,4 ± 71,4 |
| | after | 143,0 ± 56,3 | 234,4 ± 38,6 | 358,6 ± 79,8 | 454,6 ± 8,7 |
| 100 Hz | before | 124,2 ± 66,9 | 232,8 ± 95,2 | 455,8 ± 239,1 | 887,9 ± 231,2 |
| | after | 138,8 ± 56,4 | 236,4 ± 43,3 | 484,6 ± 220,3 | 716,2 ± 210,8 |
| | | | | | |
| **α-bungarotoxin** | | | | | |
| | | **amplitude** | | | |
| **frequency** | | 5 µm | 10 µm | 50 µm | 100 µm |
| 10 Hz | before | 182,5 ± 29,8 | 144,8 ± 43,9 | 162,0 ± 35,5 | 162,4 ± 36,2 |
| | after | 208,6 ± 57,4 | 191,8 ± 51,2 | 195,2 ± 52,7 | 207,4 ± 66,8 |
| 25 Hz | before | 158,8 ± 60,4 | 202,2 ± 44,6 | 206,8 ± 36,9 | 224,8 ± 0,4 |
| | after | 207,8 ± 49,3 | 203,2 ± 45,1 | 202,8 ± 44,4 | 246,2 ± 55,1 |
| 50 Hz | before | 156,2 ± 68,3 | 221,4 ± 69,6 | 344,8 ± 131,0 | 386,6 ± 88,7 |
| | after | 217,4 ± 54,0 | 355,8 ± 128,7 | 390,0 ± 119,5 | 405,4 ± 90,2 |
| 100 Hz | before | 155,6 ± 57,1 | 233,2 ± 79,4 | 385,0 ± 159,8 | 729,0 ± 290,4 |
| | after | 228,6 ± 62,2 | 378,6 ± 149,8 | 651,4 ± 303,1 | 767,0 ± 267,5 |
| | | | | | |
| **d-tubocurarine** | | | | | |
| | | **amplitude** | | | |
| **frequency** | | 5 µm | 10 µm | 50 µm | 100 µm |
| 10 Hz | before | 147,2 ± 32,4 | 137,2 ± 40,0 | 141,6 ± 40,9 | 168,6 ± 22,8 |
| | after | 152,6 ± 31,2 | 148,6 ± 39,4 | 161,4 ± 24,6 | 180,2 ± 1,0 |
| 25 Hz | before | 155,2 ± 36,0 | 198,2 ± 44,4 | 207,8 ± 36,9 | 227,0 ± 1,7 |
| | after | 170,8 ± 26,7 | 211,2 ± 28,1 | 227,4 ± 1,6 | 227,0 ± 2,1 |
| 50 Hz | before | 161,4 ± 38,6 | 223,6 ± 56,8 | 337,0 ± 99,4 | 450,4 ± 0,5 |
| | after | 181,8 ± 34,9 | 279,4 ± 97,2 | 403,0 ± 62,0 | 450,2 ± 0,4 |
| 100 Hz | before | 157,6 ± 34,7 | 227,4 ± 65,2 | 378,4 ± 91,9 | 637,8 ± 215,0 |
| | after | 178,0 ± 32,5 | 294,4 ± 92,2 | 509,2 ± 207,7 | 672,4 ± 211,5 |
| | | | | | |
| **HC-3** | | | | | |
| | | **amplitude** | | | |
| **frequency** | | 5 µm | 10 µm | 50 µm | 100 µm |
| 10 Hz | before | 190,7 ± 12,8 | 209,7 ± 7,3 | 212,3 ± 17,4 | 207,3 ± 17,9 |
| | after | 242,3 ± 65,2 | 255,0 ± 52,2 | 251,7 ± 43,9 | 267,0 ± 46,6 |
| 25 Hz | before | 183,7 ± 20,0 | 220,7 ± 8,0 | 330,3 ± 1,2 | 317,7 ± 2,0 |
| | after | 229,7 ± 60,8 | 267,0 ± 46,8 | 358,0 ± 36,1 | 365,7 ± 34,9 |
| 50 Hz | before | 174,0 ± 18,7 | 228,7 ± 82,4 | 379,3 ± 93,2 | 600,3 ± 87,0 |
| | after | 229,3 ± 60,9 | 258,7 ± 88,1 | 400,7 ± 75,8 | 656,0 ± 25,6 |
| 100 Hz | before | 181,7 ± 16,5 | 228,3 ± 73,6 | 381,7 ± 240,9 | 704,0 ± 247,7 |
| | after | 227,0 ± 71,6 | 266,7 ± 102,1 | 436,7 ± 210,7 | 826,7 ± 134,2 |